Title

Remote sensing and statistical analysis of the effects of hurricane María on the forests of Puerto Rico

Authors

Feng, Yanlei
Negrón-Juárez, Robinson I
Chambers, Jeffrey Q

Publication Date

2020-09-01

DOI

10.1016/j.rse.2020.111940

Peer reviewed

Remote sensing and statistical analysis of the effects of hurricane María on the forests of Puerto Rico

Yanlei Feng[1*], Robinson I. Negrón Juárez[2], Jeffrey Q. Chambers[1,2]

[1]*University of California, Department of Geography, Berkeley, California, USA*

[2]*Lawrence Berkeley National Laboratory, Climate and Ecosystem Sciences Division, Berkeley, California, USA*

*corresponding to: ylfeng@berkeley.edu

Received 29 July 2019; Received in revised form 7 March 2020

Remote Sensing of Environment 247 (2020) 111940

https://doi.org/10.1016/j.rse.2020.111940

Abstract

Widely recognized as one of the worst natural disaster in Puerto Rico's history, hurricane María made landfall on September 20, 2017 in southeast Puerto Rico as a high-end category 4 hurricane on the Saffir-Simpson scale causing widespread destruction, fatalities and forest disturbance. This study focused on hurricane María's effect on Puerto Rico's forests as well as the effect of landform and forest characteristics on observed disturbance patterns. We used Google Earth Engine (GEE) to assess the severity of forest disturbance using a disturbance metric based on Landsat 8 satellite data composites with pre and post-hurricane María. Forest structure, tree phenology characteristics, and landforms were obtained from satellite data products, including digital elevation model and global forest canopy height. Our analyses showed that forest structure, and characteristics such as forest age and forest type affected patterns of forest disturbance. Among forest types, highest disturbance values were found in sierra palm, transitional, and tall cloud forests; seasonal evergreen forests with coconut palm; and mangrove forests. For landforms, greatest disturbance metrics was found at high elevations, steeper slopes, and windward surfaces. As expected, high levels of disturbance were also found close to the hurricane track, with disturbance less severe as hurricane María moved inland. Results demonstrated that forest and landform characteristics accounted for 34% of the variation in spatial forest spectral disturbance patterns. This study demonstrated an informative regional approach, combining remote sensing with statistical analyses to investigate factors that result in variability in hurricane effects on forest ecosystems.

1 Introduction

Hurricanes are major natural disturbances of temperate and tropical forests in the coastal regions of North and Central America, and the Caribbean Islands (Boose *et al*. 1994, Everham and Brokaw 1996, Mabry, *et al*. 1998, McNab *et al*. 2004). The island of Puerto Rico has frequent encounters with hurricanes. Since 1700, Puerto Rico has experienced over 80 hurricanes (Boose, Foster, and Fluet 1994). Among those hurricanes, hurricane Hugo (1989) and hurricane Georges (1998) stimulated significant research on the effects of hurricane disturbance on tropical forests (e.g., Walker 1991a, Brokaw and Grear 1991, Uriarte et al. 2005). Depending on hurricane intensity and landfall duration, forest impacts vary greatly, including defoliation, small and large branches loss, and the snapping and uprooting of stems (Lugo 2008).

At the local scale, wind disturbance is influenced by forest type, stand characteristics, and tree species (Boose, Foster, and Fluet 1994: Negrón Juárez et al. 2010), and related to species adaptability, stem density, and collateral effects (Negrón Juárez et al. 2014). Different tree species vary in their vulnerability to hurricane disturbances (Zimmerman et al. 1994, Canham et al. 2010) and in their recovery pathways following wind disturbance (e.g., Walker 1991a, Zimmerman et al. 1994, Uriarte et al. 2009, Canham et al. 2010). Tree mortality is mainly due to uprooting and broken stems. Older forest stands often experience greater structural loss and basal area losses than younger stands (Everham and Brokaw 1996, Foster et al. 1999, Flynn et al. 2010).

At the landscape scale, forest change and structural loss from tropical cyclones is influenced by topography (Boose et al. 1994, Foster et al. 1999, Flynn et al. 2010). Previous studies have

shown that forests growing at high elevations and on windward slopes and ridges are more susceptible to wind disturbance (Everham and Brokaw 1996, Arriaga 2000, Bellingham and Tanner 2000, Boose *et al*. 2004). Valleys provide protection to forests from strong wind, which tends to result in lower levels of disturbance (Negrón Juárez et al., 2014). However, valleys may also amplify disturbances, as the wind can be constricted and accelerated (Everham and Brokaw 1996).

At the regional scale, significant correlations have been found between wind speed and forest structural losses (Chambers et al. 2007, Zeng et al. 2009, Negrón Juárez et al. 2014a, Schwartz et al. 2017). Wind speed decreases as a hurricane moves inland, and it decreases at larger radii from the eyewall of the storm (Boose, Serrano, and Foster 2004, Negrón Juárez et al. 2014). Wind speed is further modified by topography (Philippopoulos and Deligiorgi, 2012). Negrón Juárez et al. (2014) showed that wind speed explains 20% of the observed variation in disturbance intensity and could be used as a predictor to assess forest disturbance. Boose et al. (1994) developed a simple meteorological model, HURRECON, which combines information on the track, size, and intensity of a hurricane and the corresponding land cover to estimate wind speed. The estimated wind maps from the model supplement limited wind observations and provide high accuracy in reconstructing historical wind maps (see details in Feng et al. 2019).

Most previous studies on forest disturbance intensity were based on repeated field surveys and ground-based measurements. While these traditional approaches provide more detailed and precise local data, they are time-consuming and expensive for investigating the full extent and the magnitude of disturbance at larger scales. Due to the lack of landscape scale forest

disturbance maps, most forest disturbance studies can only explain the local disturbance variance using several factors collected from ground data. Few studies have addressed the potential for a number of mapped predictor variable layers and associated statistical analyses on forest impact variability at the landscape scale (Negrón Juárez et al. 2014). Currently, remote sensing and spatial analysis tools have rapidly developed and emerged as effective methods to investigate large-scale forest disturbance metrics after hurricanes, enabling greater insight into factors that influence spatial and temporal variation in forest disturbance and recovery processes.

Satellite remote sensing approaches can be employed to quantify the effects of forest disturbance from local to global scales and at different temporal resolutions (Frolking et al. 2009, Chambers et al. 2007, Zhu, Woodcock, and Olofsson 2012, Negrón Juárez et al. 2014, Baumann et al. 2014). Landsat imagery with high spatial resolution (30 meters) has been successfully applied to detect forest disturbances in a number of studies, and Moderate Resolution Imaging Spectroradiometer (MODIS) data with high temporal resolution (daily) enable time series analyses of hurricane disturbances (Chambers et al. 2007; Negrón Juárez et al. 2014; Helmer et al., 2010; Kennedy, Yang, and Cohen, 2010). Landsat–MODIS data fusion has become a useful method, which combines moderate spatial and high temporal resolution, to quantify and explain some of forest disturbance patterns (Chambers et al., 2007; Hilker et al., 2009; Xin et al., 2013; Negrón Juárez et al., 2014). However, few researchers have carried out landscape-scale studies on the factors which affect the spatial distribution of these disturbance patterns. Moreover, traditional ground-based field validations are time-consuming and costly. High spatial resolution data, such as Panchromatic IKONOS with 1-meter resolution and QuickBird satellite data with 0.7-m resolution, has been used to quantify local tropical forest mortality (Frolking et al., 2009;

Clark et al., 2004). In this study, we used high spatial resolution airborne images to assist in validating larger-scale forest disturbance patterns.

Hurricane María made landfall in Puerto Rico on September 20, 2017, as Category 4 hurricane on the Saffir–Simpson scale (Pasch et al. 2018), producing unprecedented forest disturbance in Puerto Rico (Uriarte et al. 2019). In this study, we use satellite imagery to quantify the effects of hurricane María on forests in Puerto Rico, and analyze a large number of landscape-scale factors that affect the spatial variance in forest disturbance. The use of Google Earth Engine (GEE) (Gorelick et al, 2017) allowed us to combine data from different sources, including observations from satellite and aerial imaging systems, topographic, land cover, and GIS datasets, for a comprehensive understanding on the effects of Hurricane María on Puerto Rico forests. The objectives of this study were to:

1) Develop a GEE remote sensing data analysis tool for rapidly quantifying spatial variability in forest disturbance following a hurricane landfall;

2) Study the landscape factors that affect the patterns and severity of forest disturbance intensity;

We also developed a number of user interfaces tools to share our results, which allow a larger community with access to maps and analysis tools for the hurricane affected area.

2 Study area

The island of Puerto Rico is located in the Caribbean (centered at 18.2°N, 66.4°W). Forests cover about 60% of Puerto Rico, and all the forests fall within the subtropical belt of Holdridge Life Zone System (Holdriodge 1967, Harris et al. 2012). The forest types vary widely, including drought deciduous forests, semi-deciduous forests, seasonal evergreen forests, and evergreen

forests. The wettest forest types are found at higher elevations, while the driest forest types are in southern and southwestern Puerto Rico. Hurricanes are the primary natural disturbance causing widespread impacts to ecosystems and human livelihoods (Miller and Lugo 2009).

3 Hurricanes

In the past 50 years, two major hurricanes hit Puerto Rico, reaching up to 175 km h^{-1} maximum wind speed. Past hurricanes and minor storms affected ecosystems, human populations, and infrastructure (see summary of effects in Tanner *et al.* 1991). Following Hurricane Irma, Hurricane María made landfall near Yabucoa Harbor, Puerto Rico with the maximum sustained wind speed around 250 km h^{-1}. This research focused on the combined effects of these two hurricanes in extreme active 2017 hurricane season, with an emphasis on Hurricane María.

4 Data and Methods

4.1 Multi-spectral Remote Sensing Data

Landsat 8 Operational Land Imager and Thermal Infrared Sensor (OLI/TIRS) surface reflectance data were used in this study. To represent the pre-disturbance period images from June 1, 2016 to September 30, 2016 were used, and the for the post-disturbance period images from October 1, 2017 to January 30, 2018. Only images with less than 40% cloud cover were used. The two slightly different time periods were chosen to generate cloud-free pre and post hurricane images that cover most of the island and try to minimize the bias associated with seasonal phenology. All the remote sensing images were identified, processed, and analyzed using Google Earth Engine (Gorelick et al. 2017).

Images from Landsat 8 Surface Reflectance have been atmospherically corrected using Landsat 8 Surface Reflectance Code (LaSRC) to meet geometric and radiometric quality requirements. Cloud and shadow mask were created using the data quality assessment band (BQA) in Landsat 8 and applied to the images. Post-hurricane images were radiometrically calibrated and topographic illumination corrected (see Feng et al. 2018 for details). The overlapping images were composited according to their cloud cover with the least cloudy images on the top. Two false color remote sensing images for the pre-hurricane (Figure 3a) and post-hurricane periods (Figure 3b) were generated.

4.2 Landform characteristics

Hurricane wind speed is the main driver of affecting the severity of forest disturbance. However, on land hurricanes wind speeds are affected by (1) elevation (Luo et al., 2008; Boose, Foster, and Fluet, 1994), (2) slope, (3) distance from the landfall of the storm (Irish et al., 2008; Powell, 1982; Luo et al., 2008), (4) distance from the hurricane track (Boose, Foster, and Fluet, 1994; Irish et al., 2008; Gannon and Martin, 2014; Xi et al., 2008), and (5) windwardness as a proxy for aspect exposure (Pouteau and Stoll, 2012; Boose, Foster, and Fluet, 1994). We explored how these landform affected forest disturbance.

The Shuttle Radar Topography Mission (SRTM) digital elevation dataset (Jarvis, Reuter, Nelson, and Guevara, 2008) was used to characterize landforms affected by hurricanes in Puerto Rico. The slope and aspect data were generated on the basis of the elevation data. The track of hurricane María was acquired from the National Tropical Center, NOAA. We assumed that hurricane María's landfall line was perpendicular to its track, so each point on the parallel line to the landfall line had the same distance. The data regarding the distance from the hurricane

landfall (LFproximity) and the distance from the hurricane track (HTproximity) were then generated using the ArcGIS 10.6 Euclidean distance function in the spatial analysis tool (Environmental Systems Resource Institute, ESRI, Redlands, California).

Aspect and hurricane track direction, were transformed into a windwardness index (Fig. 1). We assumed that the wind along the hurricane track had the maximum wind speed, so the area with a southeastern aspect facing the strongest wind was assigned the highest windwardness index of 180. Inversely, the windwardness of the leeward side was 0.

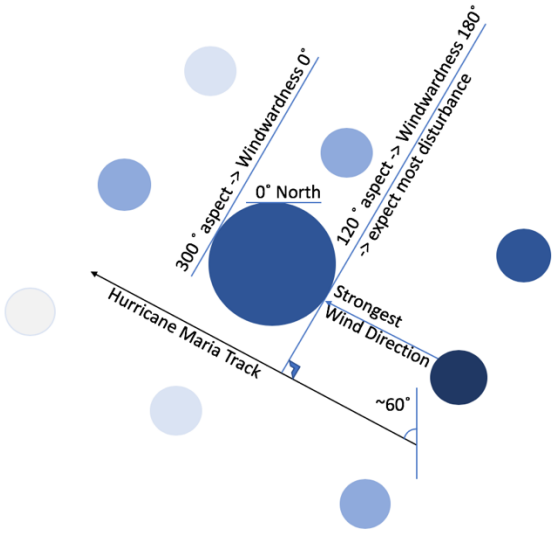

Fig. 1 Transformation of the windwardness indexes from aspects. Darker blue represents higher wind speed.

4.3 Forest Structure Data

The forest canopy dataset was based on a fusion of spaceborne lidar data (2005) from the Geoscience Laser Altimeter System (GLAS) and ancillary geospatial data (Simard et al., 2011). The Puerto Rican forest types and forest age class data were produced based on Landsat imagery

classification, aerial photo interpretation, and time series map analysis (Helmer et al., 2002; Helmer and Kennaway., 2007; Helmer et al., 2008).

4.4 Spectral Mixture Analysis

To map forest disturbance severity produced by Hurricane María, we conducted spectral mixture analysis (SMA) (Adams et al. 1995; Shimabukuro and Smith 1991) on Landsat composites. SMA quantifies per pixel fraction of each endmember (Adams et al. 1995), including green vegetation (GV), non-photosynthetic vegetation (NPV), and shade (see Feng et al. 2018 for details). Our focus was only on the forested areas, and hardly any bare ground was observed in the forests through the remote sensing images, so no soil endmember was included. The GV endmember was selected using the pre-cyclone images. The NPV endmember was easily recognized and obtained in the post-cyclone images, because exposed wood and surface litter showed high values in middle infrared reflectance band. The shade endmember was obtained using the spectra of water (Adams and Gillespie, 2006) to account for the effects that related to the view angle, topography, shading, and shadows (Adams and Gillespie, 2006; Roberts, Adams, Smith, 1993). The shade proportion was removed by re-summing GV and NPV to 1 (Adams and Gillespie, 2006). After this normalization, the changes in NPV (ΔNPV) were calculated as NPV post-hurricane María minus NPV pre-hurricane María (Fig. 4b), which provides a quantitative measure of the changes in the dead vegetation, woody biomass, and surface litter associated with the hurricane disturbance (Chambers et al. 2007, Negrón Juárez et al. 2011, Feng et al. 2018).

4.5 Time series of the enhanced vegetation index (EVI)

We used the time series of the EVI across the island for the temporal analysis of hurricane María's effects on the forested ecosystem . EVI is a vegetation index with increased sensitivity in heavily vegetated areas. Therefore, the forested areas affected by hurricane María were expected to show low values of EVI. We determined if these values were in the range of the interannual variability of EVI in Puerto Rico. The MODIS EVI product was calculated as EVI=G*(NIR-RED) / (NIR+ a*RED-b*BLUE+L) (Justice et al. 1998; Huete et al., 2002). EVI is appropriate for tracking tropical forest disturbances (e.g., Huete et al. 2002, Huete et al. 2006). We generated a time series of MODIS EVI to determine the temporal severity of the forest disturbance caused by hurricane María compared with other events during the study period in Puerto Rico.

4.6 Google Earth Engine Platform

Google Earth Engine (GEE) (Gorelick et al. 2017) has enabled high-performance, parallel remote sensing analyses. Large numbers of geospatial datasets can be found on its cloud-based platform, and associated remote sensing tools can be accessed using JavaScript API. GEE makes it easy to access powerful computing resources for processing very large datasets without shouldering the IT burden. Its web-based interactive development environment is suitable for demonstrating and sharing the visualization of results (Gorelick et al., 2017). GEE has been used in a wide variety of disciplines. It can provide sufficient computing power in global land use and land cover change studies (Hansen et al., 2013; Pekel et al., 2016). GEE can also be used for regional studies, including quick assessments of natural disaster mapping (Coltin et al., 2016) and disease risk mapping (Sturrock et al., 2014).

4.7 Regression Analysis

Statistical analyses were conducted in R v. 3.4.4 (R core team, 2013). A series of full and reduced linear regression models were developed to analyze the effects of the forest structure and the landform characteristics on the hurricane disturbance. First, a series of simple linear regression models were built by analyzing the disturbance and the factors of elevation, slope, aspect, windwardness, distance from the hurricane track, distance from the landfall, forest age, forest types, and the pre-hurricane GV ratio, individually. Then, a multiple linear regression model was constructed by entering the forest disturbance (represented by ΔNPV) as the dependent continuous variable, and all the factors were entered as independent variables. The forest age variable was converted into interval scales by extracting the median from each forest age category. While all the other variables were continuous, the forest type was calculated as a categorical variable in the regression. A sample of 50,000 pixels (1.44 % of the total 3,480,048 pixels) was used in the analysis. A total of 1446 pixels (2.89% of the total sample) were identified as outliers and removed based on their extremely large Cook's distances, which indicated pixels overly influential to the regression results. These outliers can result from misclassification of forested pixels, atmospheric scattering, and topographic illumination. The Student's t-test was performed to test the null hypothesis H_0 that there is no difference between the forest disturbance for each of the factors. The P value was calculated to test the significance level of the factors. The significance level was set at $\alpha = 0.05$. Relative importance was computed to calculate the proportionate contribution each independent variable makes to R^2.

4.8 G-LiHT derived disturbance

High-resolution (3-4 cm ground resolution) images were captured using Goddard's LiDAR, Hyperspectral & Thermal Imager (G-LiHT) by NASA (Cook et al. 2013) before (March 2017) and after hurricane Irma and hurricane María hit Puerto Rico (March 2018). High resolution RGB images from the G-LiHT aerial photography platform were used to derive comparable ΔNPVs as ground validation data for Landsat-derived ΔNPV forest disturbance map. First, we chose 4 regions where G-LiHT RGB images were georeferenced with minimal shade across the island. Then 4 Landsat pixel size samples -- 30 by 30 meters -- were selected for each region, with 16 squares in total chosen. Next, pre- and post-hurricane G-LiHT images were clipped to these squares, so we had 32 high-resolution images at four total sites (Figure S1). We manually chose training samples of vegetation, non-photosynthetic vegetation, and shade from each RGB image. We then carried out a supervised classification using a maximum likelihood method. After classification, normalized ΔNPV from G-LiHT RGB images were calculated and compared with Landsat-derived normalized ΔNPV at for the same locations (Fig. 13).

5 Results

5.1 Effects of María on Puerto Rico

An analysis of the MODIS-EVI (Fig. 2) quantified the temporal effects of hurricane María on the forests of Puerto Rico. Comparing to mean EVI since 2000 (black lines in Fig. 2), EVI for Puerto Rico during the hurricane season of 2017 showed a sharp decline in vegetation greenness (orange line in Fig. 2). A rapid decline on September 13 and a much steeper decline in the subsequent interval up to September 29 in the EVI of 2017 (green line in Fig. 2) shows the effect of

hurricane Irma and hurricane María's landfall and traversing of the island (Feng et al. 2018). Even though EVI recovers from the deep decline caused by the hurricanes, the average EVI of the wet season (from May to October) in 2018 is still 6.5% lower than mean EVI for the past 20 years and 5.0% lower than that of 2017 before the hurricanes, indicating the existence of severe tree disturbance that required more than one year to recover.

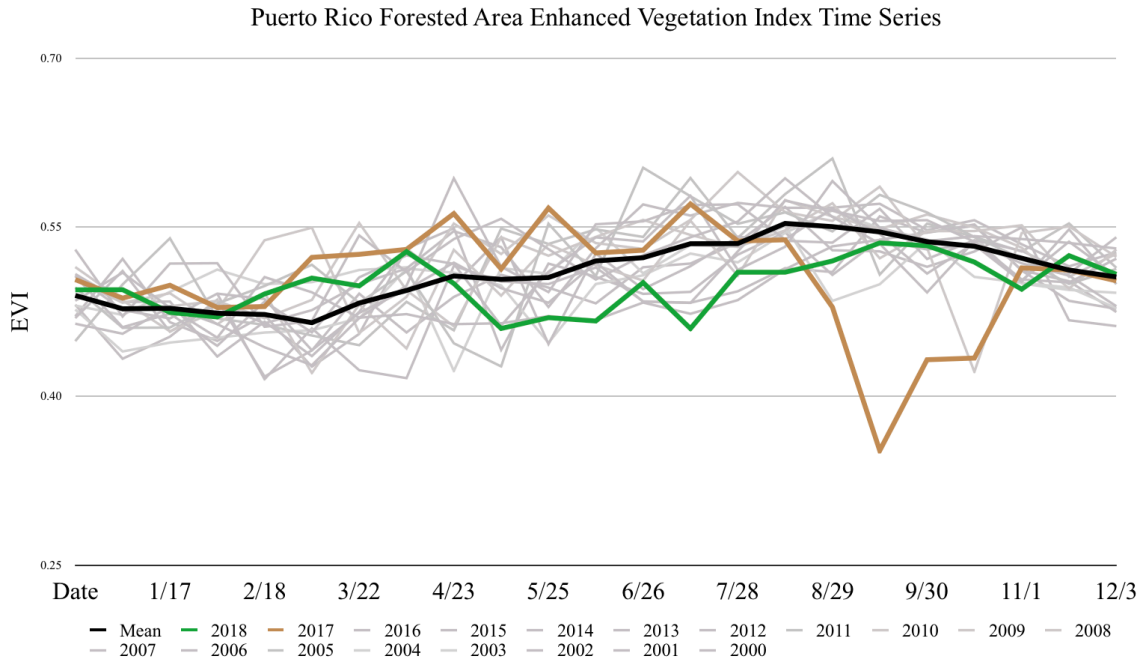

Fig 2 -- Average time series of MODIS-EVI from the forested pixels across Puerto Rico during 2000–2018, showing an immediate spectral shift following hurricane María's landfall and the subsequent recovery as the surviving trees flushed out new leaves.

The pre- and post-hurricane María images clearly illustrate a major shift in color from green (NIR) to reddish (SWIR) (Fig. 3a and 3b, respectively), representing the widespread forest disturbance (see detailed explanations in Feng et al. 2018). The images were visualized as band 6

(SWIR) shown in red, band 5 (NIR) shown in green, and band 4 (red) shown in blue. In this way, forest impacts can be readily identified compared with the true-color images.

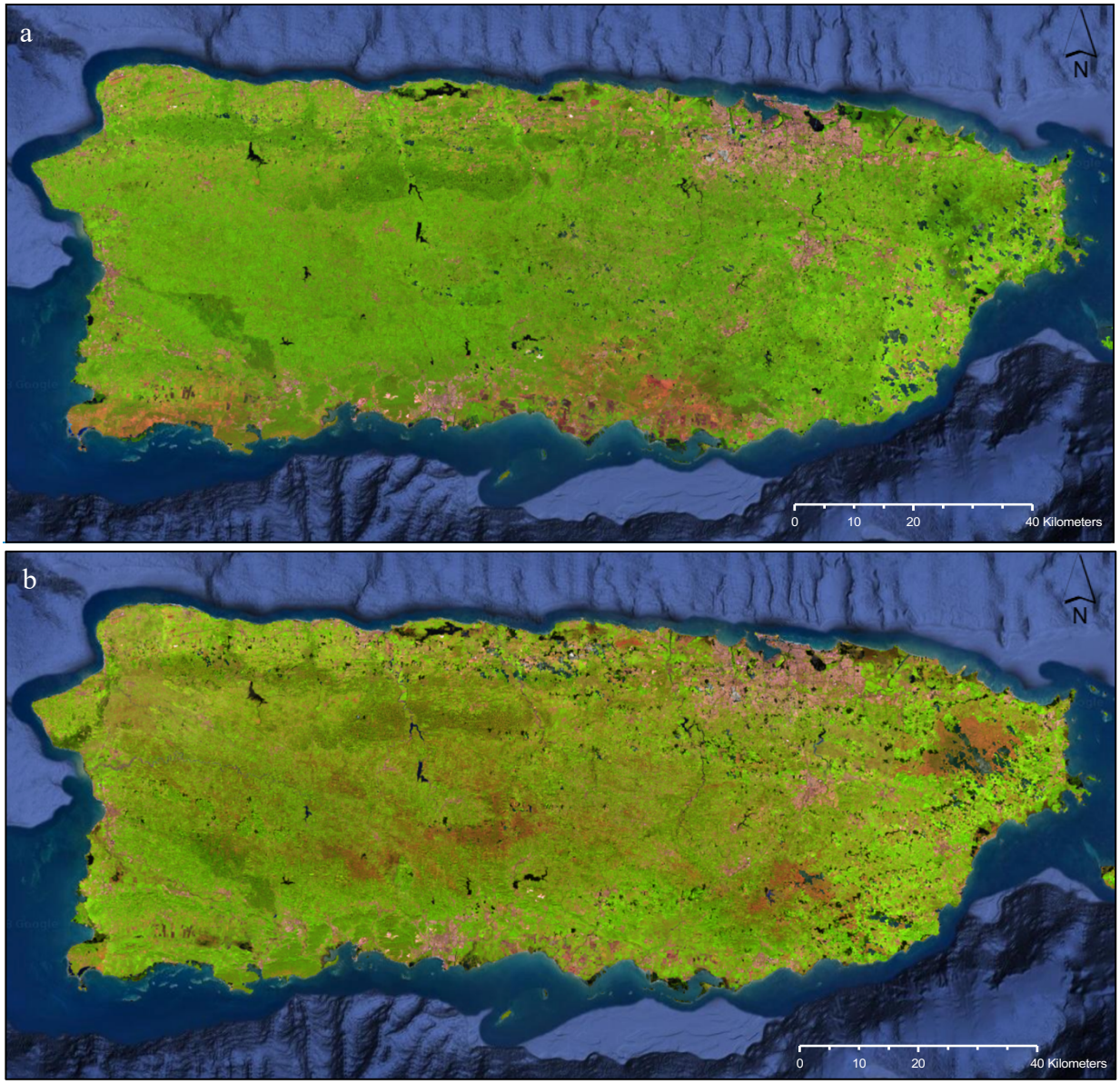

Fig 3 –a) Pre and b) post hurricane María Landsat 8 false-color image of Puerto Rico, centered at 18.20°N, 66.48°W, with the following display colors: red: SWIR band, green: NIR band, and blue: red band. SWIR: short-wave infrared; and NIR: near-infrared.

The sensitivity of the multispectral data associated with the forest disturbance was quantified and demonstrated in color ΔNPV maps (Fig. 4). A decreasing trend of forest disturbance can be observed from ΔNPV maps generated one month (Fig. 4a), four months (Fig. 4b), and one year (Fig. 4c) after hurricane María. Fig. 4a shows that most of the forested area is covered in red, which represents very high disturbance intensity across the island. Fig. 4b clearly shows the heavily affected forests while other forested areas were recovering. Fig. 4c shows that most of the forested area have negative ΔNPV, indicating new leaves coming out. We chose the ΔNPV map four months after hurricane María (Fig. 4b) which best represent the major hurricane impact on forest for the following analysis and calculating mortality rate in the future. High ΔNPV in red colors (black, brown, and red) indicates high levels of tree mortality and tree structural loss, including defoliation, loss of branches, and snapping and uprooting. Highest forest disturbances occurred in Luquillo Mountains, the mid-west forested area, the southeastern area, and the northeastern coastal area.

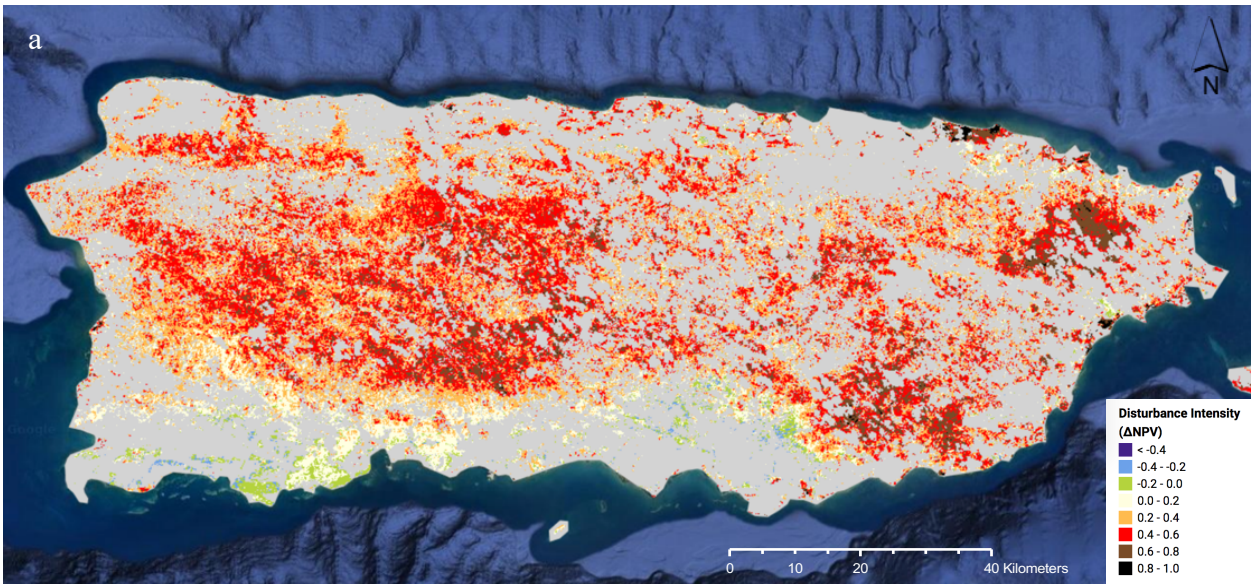

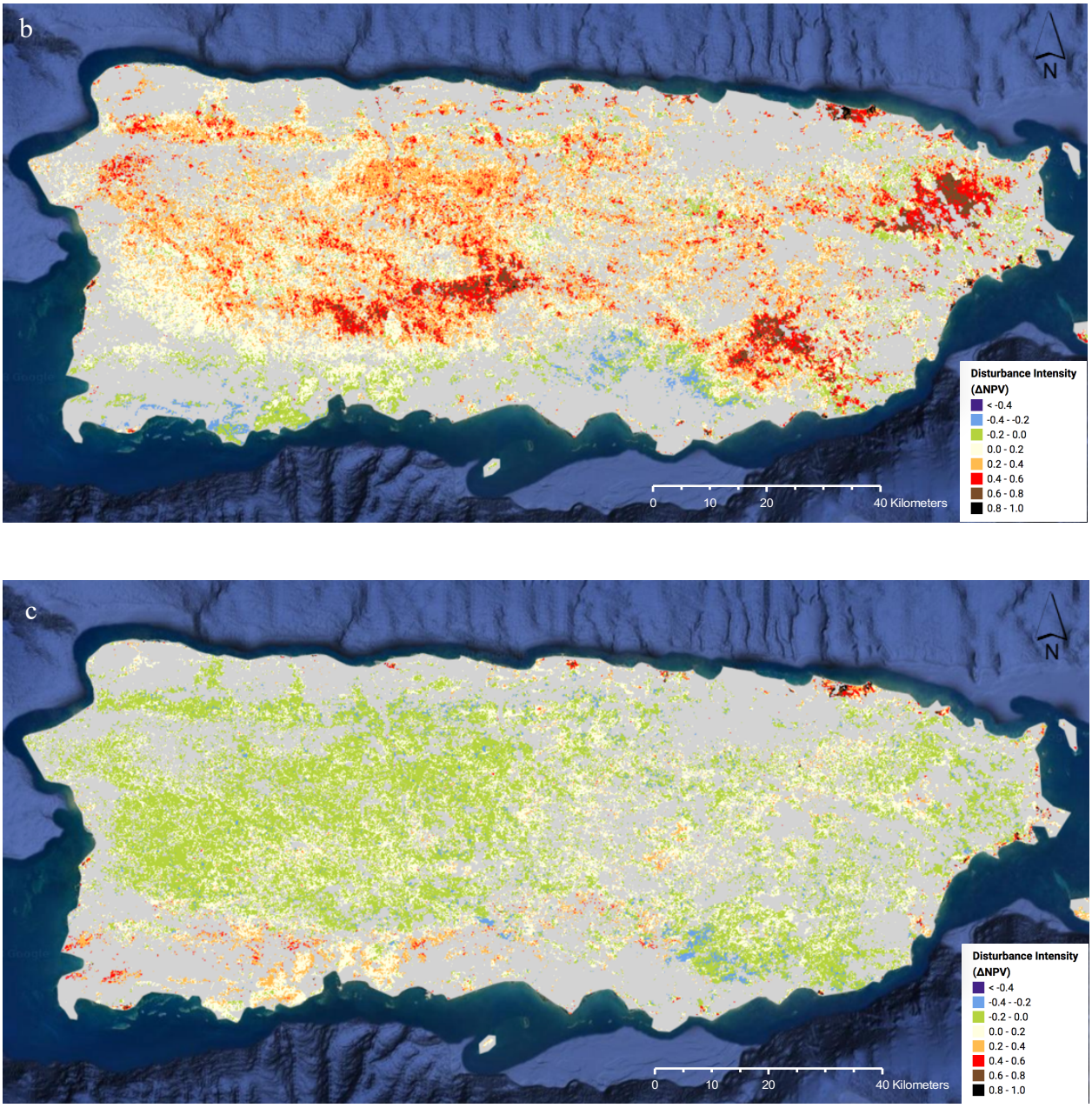

Fig 4 -- ΔNPV map of Puerto Rico forested pixels a) one-month b) four months c) a year after Hurricane María. Hurricane Irma had residual effects on the north-east region.

The highest forest disturbance intensity is colored in darker tones of red, indicating defoliation, snapped and wind-thrown trees. The grey areas represent non-forested areas or cloudy areas. The datasets for all the images are available here: http://dx.doi.org/10.15486/ngt/1419953.

Significant variation in the ΔNPV disturbance signal indicates a number of factors driving the spatial variation of the forest effects of hurricane María. In the following sessions, we conducted a regression analysis to find the factors that control the variability in the forest vulnerability.

5.2 User Interface tools

We also used GEE packages to build two client-side user interfaces (UI). The user can choose an image from among the pre-María, post-María, and forest disturbance intensity images to visualize in the first UI (Fig. 5a, see detailed description in Feng et al. 2018). The second UI (Fig. 5b) has split panel so that users can compare before/after hurricane imagery and forest disturbance intensity with a variety of time periods.

a

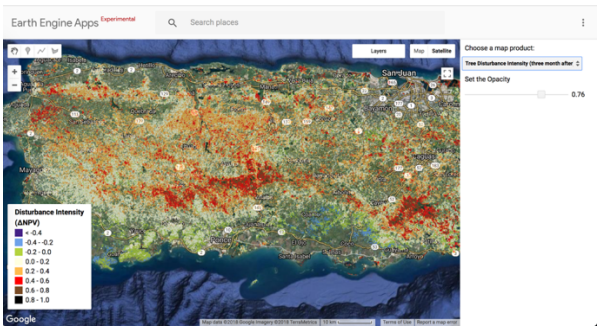

b

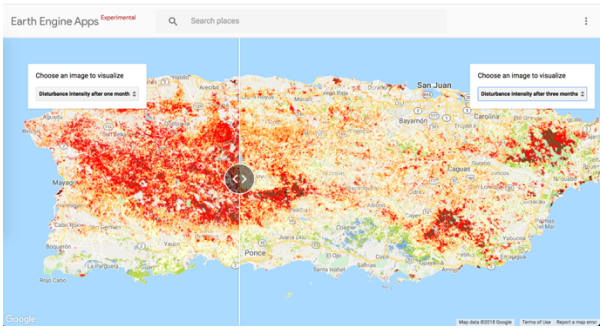

Fig 5. Google Earth Engine published apps publicly available at (a) https://ylfeng.users.earthengine.app/view/forestdisturbancemapinpr and (b) https://ylfeng.users.earthengine.app/view/forestdisturbanceafterhurricaneMaría.

5.3 Effects of landforms on forest disturbance

The effect of the intensity of the storm on the Landsat-derived disturbance values associated with hurricane María was investigated. Fig. 6 shows the association between the forest disturbance and the terrain features, including slope, elevation, and windwardness. Forest disturbance was highly correlated with elevation ($p < 0.001$) but did not vary significantly with slope. Disturbance increased with the increasing elevation. Less than 5% of the forests were on land with an elevation above 800 m and had an average ΔNPV of 0.43. Elevation alone explained 6.2% of the forest disturbance variance.

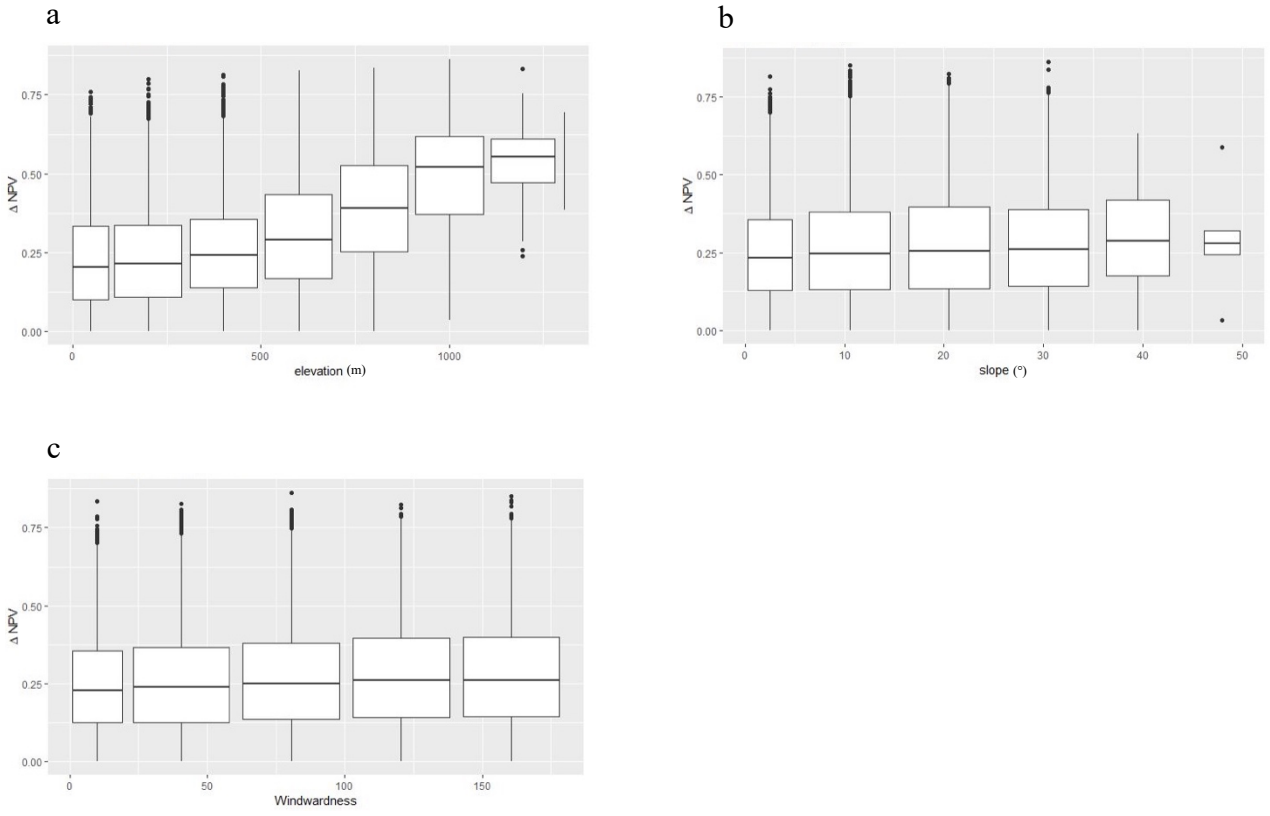

Fig 6. The variation of the disturbance ΔNPV with respect to terrain (a) elevation, (b) slope, (c) windwardness in box plots.

The track of hurricane María was from southeast to northwest, around 300° (WNW). Surfaces with aspects (90–150°) varying at ±30° perpendicular to the direction of the storm motion were on the windward side and highly susceptible to topographic accelerations. The lowest disturbance was observed on the surface with aspects around 300–340°, which was on the leeward (topographic sheltered) side with respect to the direction of the hurricane track. Therefore, we introduced a windwardness index as a proxy for the southeastern wind exposure. ΔNPV was positively correlated with windwardness (Fig. 6c), and forests on the eastern side of the hurricane track showed a stronger relationship than those on the western side.

On the west side of the storm, a continuous high disturbance occurred within approximately 40km of the hurricane track (Fig. 7a). Then, the forest disturbance decreased as the distance from the center of hurricane (HTproximity) increased. On the east side of the hurricane, high forest disturbance was found in forests of the Luquillo Mountains (showing in orange colors in Fig. 7b). Other forested pixels on the west side of the track showed similar decreasing disturbances as the distance from the hurricane track increased. Therefore, we created an interactive variable HTproximity * WestEast. The WestEast variable has 0 on the west side of the hurricane track and has 1 on the east side. We also added HTproximity*windwardness in the regression. All of these variables were significant in the regression analysis ($p < 0.001$) and explained 5.3% of the forest disturbance variance.

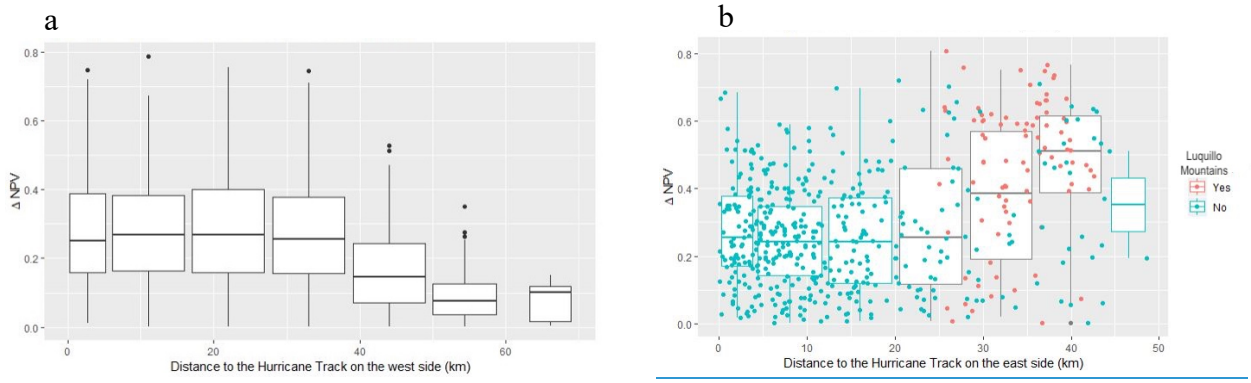

Fig 7. The variation of the disturbance (ΔNPV) with respect to the distance to the track of hurricane María on the (a) west side and (b) east side. In figure b, orange points are located in Luquillo Mountains, while cyan points are not.

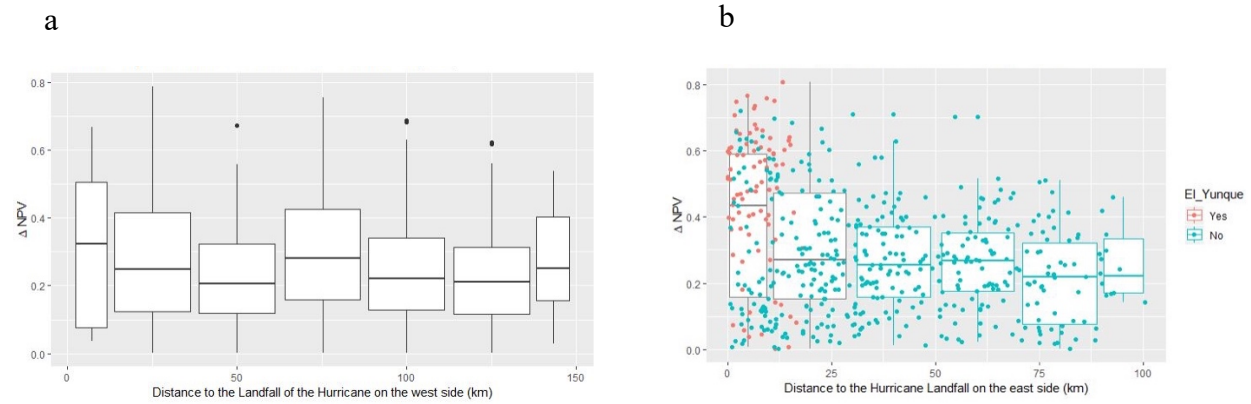

Fig 8. The variation of the disturbance (ΔNPV) with respect to the distance from the landfall of hurricane María on (a) the west side and (b) the east side. The distance is calculated as the Euclidean distance from the point to the landfall line which is perpendicular to the hurricane track.

María produced the maximum forest disturbance in the southeastern coast, where the hurricane made landfall, and the Luquillo Mountains. The forest disturbance decreased as the storm moved onshore on the east side of the track (Fig. 8). On the west side, the forest disturbance intensity has a decreasing trend as the hurricane move inland. The maximum ΔNPV was closest to the

place where hurricane María made landfall. ΔNPV was found relatively high at 75km from the landfall, which might be due to the combination factors of high elevation and steep slope.

5.4 Effects of forest type on disturbance

The Landsat-derived forest disturbance varied across the different forest types. The elfin and sierra palm cloud forests (29); sierra palm, transitional, and tall cloud forests (18); mangrove forests (21); and seasonal evergreen forests with coconut palm (15) emerged as the most affected forest types, with average ΔNPV values larger than 0.4 (Fig. 9). All these forest types were positively correlated with forest disturbance. These forest types were mainly located in the center of Luquillo Experimental Forest (LEF), Toro Negro Commonwealth Forest, Carite Commonwealth Forest, and the northeastern and southern coasts. Semi-deciduous and drought deciduous forests on alluvium and non-carbonate substrates (10), semi-deciduous and drought deciduous forests on karst/limestone (including semi-evergreen forest) (11), and drought deciduous, semi-deciduous, and seasonal evergreen forests on serpentine (12) emerged as the most resistant forests, which had an average ΔNPV of less than 0.2. Seasonal evergreen and evergreen forests (14), the main forest type (64%, Kennaway and Helmer, 2007) in Puerto Rico, varied the most with respect to the forest disturbance, with an average ΔNPV of 0.265. The forest type variable explained 9.5% of the variance in the forest disturbance.

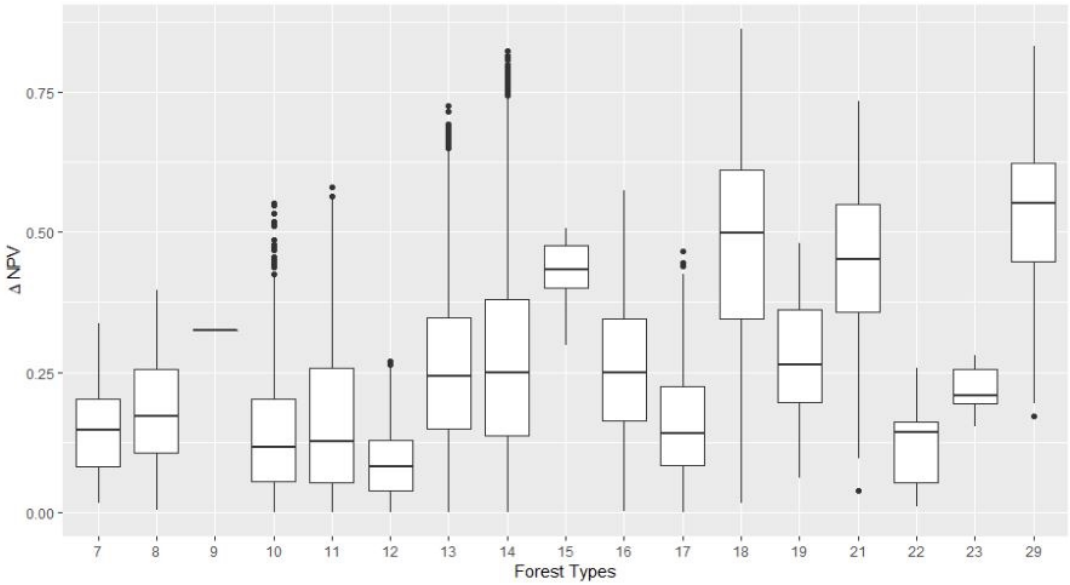

Fig 9. The variation of the forest disturbance (ΔNPV) with respect to different forest types. The forest types are listed below:

7 Drought Deciduous Open Woodland

8 Drought Deciduous Dense Woodland

9 Deciduous, Evergreen Coastal and Mixed Forest or Shrubland, with or without Succulents

10 Semi-Deciduous and Drought Deciduous Forest on Alluvium and Non-Carbonate Substrates

11 Semi-Deciduous and Drought Deciduous Forest on Karst/limestone (includes semi-evergreen forest)

12 Drought Deciduous, Semi-deciduous and Seasonal Evergreen Forest on Serpentine

13 Seasonal Evergreen and Semi-Deciduous Forest on Karst

14 Seasonal Evergreen and Evergreen Forest

15 Seasonal Evergreen Forest with Coconut Palm

16 Seasonal Evergreen and Evergreen Forest on Karst

17 Evergreen Forest on Serpentine

18 Sierra Palm, Transitional and Tall Cloud Forest

19 Emergent Wetlands Including Seasonally Flooded Pasture

20 Salt or Mud Flats

21 Mangrove

22 Seaonally Flooded Savannahs and Woodlands

23 Pterocarpus Swamp

29 Elfin and Sierra Palm Cloud Forest

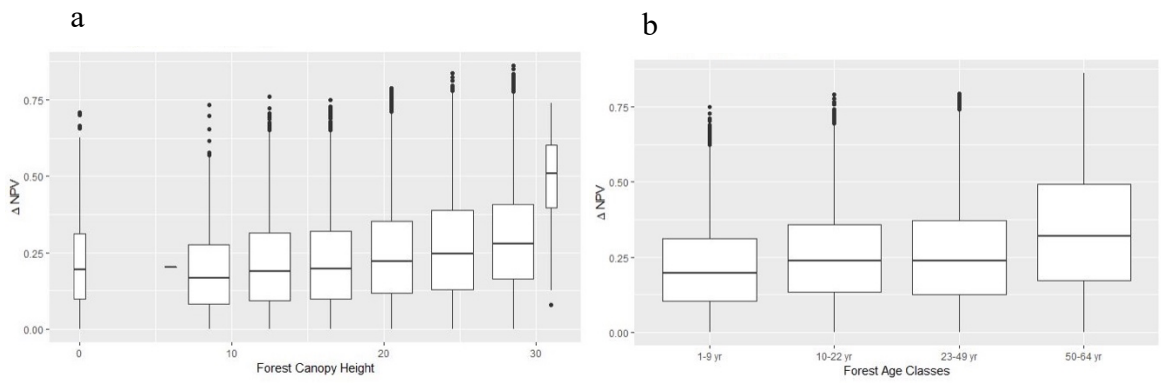

Fig 10. The variation of the forest disturbance (ΔNPV) with respect to (a) forest canopy height and (b) forest age.

Fig. 10a shows the association between the forest disturbance and the forest canopy height (standard coefficient (SC) = 0.055, p <0.001). Taller trees were more vulnerable to hurricane María. Fig. 10b shows that the age class had a significant effect on the forest disturbance (p <0.001), and the oldest forests (50–64+ years) showed the greatest effect. Trees aged 50–64+ had the highest average ΔNPV of 0.306, while young sites had the lowest average ΔNPV of 0.258. The age class variable predicted 2.5% percent of the variance in the forest disturbance.

5.5 Landsat-derived disturbance and green vegetation ratio in the preceding year

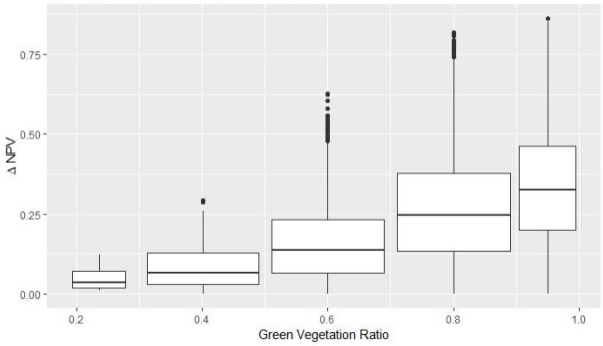

Fig. 11. The variation of the forest disturbance (ΔNPV) with respect to the green vegetation ratio of forested area in 2017.

The green vegetation ratio of Puerto Rico's forested area in 2016 represents the fraction of the vegetation cover in each pixel. It showed a strong positive correlation with the forest disturbance (Fig. 11). The majority of the forested pixels had over 70% forest cover. This independent variable contributed to 7.4% of the explained variance.

5.6 Full regression model and Relative importance

A multiple linear regression analysis was performed, and the results from the model showed that all the factors in Table 1 were highly significant in explaining variation in forest disturbance caused by hurricane María ($P < 0.001$, respectively). In the standard coefficient test, the interactive variable of the distance to the hurricane track and the side of the track (Standard Coefficient = 0.38), forest type (seasonal evergreen and semi-deciduous forest on karst (SC = -0.321)), elevation (SC = 0.274), green vegetation ratio in 2016 (SC = 0.275), distance to the landfall (SC = 0.240), and distance to the hurricane track (SC = -0.211) had the highest standardized beta coefficients. Annual precipitation was also tested as a factor in the model and it was not significant, so it was removed. The P value for the multivariable regression also showed significance ($P < 0.001$***). Forest type, green vegetation in 2016, and elevation had the highest contribution to R^2, which explained most of the disturbance variance. Overall, 34.5% of forest disturbance variance was explained by these factors. The residuals from the final fitted models were normally distributed. No extreme multicollinearity was present between the independent factors in this model (general variance inflation factor (GVIF) ≤7, respectively) (James et al., 2013; Fox and Monette 1992).

Table 1 The multivariable regression examining the correlation between the forest disturbance (ΔNPV) and all the variables in Puerto Rico.[a]

Independent Variable	SC	SE	*T*	*P*	*R*
Elevation	0.274	4.544e-06	45.256	<0.001***	0.062
Slope	-0.041	9.625e-05	-9.898	<0.001***	0.002
Windwardness	0.095	2.237e-05	14.354	<0.001***	0.005
ForestCanopyHeight	0.054	1.329e-04	11.661	<0.001***	0.013
HTproximity	-0.211	2.152e-04	-22.160	<0.001***	0.010
LFproximity	0.240	6.904e-05	24.574	<0.001***	0.016
Forest Type*	-	-	-	-	0.095
GV2016	0.275	8.445e-03	73.215	<0.001***	0.074
Age	0.147	3.661e-05	34.038	<0.001***	0.025
HTproximity:WestEast	0.382	2.389e-04	44.634	<0.001***	0.038
HTproximity:windwardness	-0.108	1.410e-06	-11.991	<0.001***	0.005

[a]N = 50000, HTproximity = Distance to hurricane track, LFproximity = Distance to hurricane landfall, SC = standard coefficient, SE = standard error, t = t value. *P* = significance, *R* = R^2 statistic (relative importance metrics). Multiple R^2 = 0.34, Adjusted R^2 = 0.34

*Table S1

5.7 Validation

Normalized G-LiHT RGB ΔNPV was used to validate Landsat-derived ΔNPV produced from the same time periods as G-LiHT images were taken.

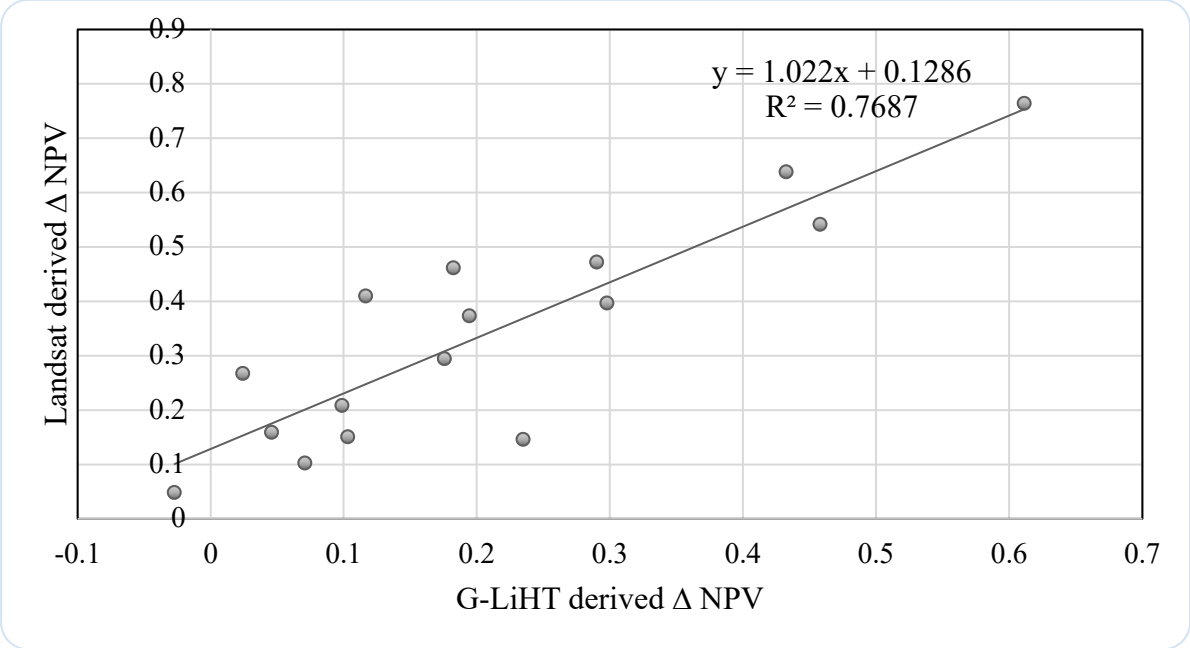

Fig. 13 Relationship between G-LiHT ΔNPV and Landsat ΔNPV at sixteen locations in Puerto Rico.

The figure shows a positive relationship between G-LiHT ΔNPV and Landsat ΔNPV. A linear function was used to fit the relationship. A high R square (0.77) indicates a strong relationhips between Landsat ΔNPV and high-resolution G-LiHT RGB ΔNPV representing useful ground validation approach when lacking suitable field-based data. 23% of Landsat ΔNPV was not explained by the G-LiHT ΔNPV, and a factors might explain that unexplained variability include underestimation of vegetation area due to different sizes of shade area within forests, and classification errors caused by manually selecting training samples.

6 Discussion

6.1 Tree mortality and recovery

Previous studies have shown that an increase in the Landsat-derived ΔNPV of the same area after tropical cyclones is positively and linearly correlated with field-measured tree mortality and extensive crown effects (Chambers et al., 2007; Negrón Juárez et al., 2014a). This strong correlation between the shift in the spectral reflectance and tree mortality and canopy disturbance has enabled quantitative measurements of tree mortality using remote sensing images. Chambers et al. (2007) developed a Monte Carlo model to estimate the tree mortality caused by hurricane Katrina based on this correlation. Similar approaches to calculating tree mortality, stem density, and biomass distribution have been applied to other landfalling hurricanes in the US (Negrón Juárez et al. 2014a) and Australia (Negrón Juárez et al. 2014b) and strong convective storms affecting Amazon forests (Negrón Juárez et al. 2010). Based on remote sensing and the fieldwork carried out regarding landfalling hurricanes in US forests, tree mortality may be related to the stem density (Negrón Juárez et al. 2014a). Using Forest Inventory and Analysis (FIA) data over Puerto Rico we estimated that the initial order-of-magnitude effects of hurricane María on the trees, including tree structural effects and mortality, was around 23–31 million trees (Feng et al., 2018). However, it is challenging to determine what fraction of trees are dead in satellite images at 30-meter resolution. Moreover, even trees that have lost their crowns and a portion of their height can regrow canopies and live productively (Lugo 2018). Improved tree mortality maps and numbers will require on fine resolution airborne images, field-measured mortality rates, and stem density.

Rapid forest recovery after hurricane María was shown in the time series of the EVI. After a sudden and deep decline in the EVI of the forested area in Puerto Rico in September, it took two months for the EVI to partially bounce back. Similar patterns have been observed in previous studies. New leaves were observed within a few weeks to a few months (Everham and Brokaw 1996, Walker et al. 1992). A rapid rate of forest recovery after hurricanes was observed in the Luquillo Mountains (Lugo 2018, Lugo et al. 2015). The observed tree mortality was 4% of all the upright trees despite high levels of snapped (85%) and uprooted (77%) trees in Walker's study of the effects of hurricane Hugo in LEF in Puerto Rico (Walker 1991a). In the Luquillo Mountains, frequent disruption from hurricanes results in a number of strategies for trees in response to these disturbances, and these varied responses enable forests to resist or recover when confronted the recurrent hurricanes (Lugo et al. 2015). EVI of Puerto Rico forests in 2019 shows that spectral recovery continues. Several studies have suggested a 5 to 10-year reorganization period before the recovery mechanics are fully operational, which may include delayed mortality (Everham and Brokaw 1996). Estimates of tree recovery time varies tremendously by different quantification of recovery, frequencies of disturbance, and tree species (Everham and Brokaw 1996; Walker 1991a). Future more continuous field measurements are needed to provide more accurate estimates of tree mortality and tree damage in synergy with remote sensing and geospatial analysis.

6.2 Landforms and forest disturbance

Our results showed that Landsat-derived forest disturbance was positively correlated with elevation, slope, and windwardness (calculated from aspect and the hurricane direction), and was negatively correlated with the distance from the hurricane track and landfall. The Landsat-

derived disturbance showed high disturbance in the windward areas and low disturbance in the leeward areas. This correlation has been described in previous studies (Lugo and Frangi, 2016; Negrón Juárez et al., 2014; Xi et al., 2008; Boose, Serrano, and Foster, 2004). While windward slopes are subjected to more intense winds, they are also preconditioned by chronic winds from the same direction in some cases. Therefore, hurricane effects to the structure of cloud forests at high elevations in Puerto Rico did not vary between windward and leeward sites (Brokaw and Grear 1991; Boose et al. 1994), and the overall positive correlation between windwardness and disturbance intensity is weak. The forests on the east (lee) side of hurricane had more disturbance than that on the west side. Due to the motion of the hurricane contributing to its rotation, hurricane María, as a counter-clockwise rotated hurricane in the northern hemisphere, should have had higher wind speeds on the right side than on the left side (Negrón Juárez et al., 2014; Boose, Serrano, and Foster, 2004), which may explain the differences in the forest disturbances on the two sides of the hurricane. In addition, hurricane María made landfall near the southeastern coast, meaning that the forests in the surrounding areas suffered more due to strong wind. Forests on the lee side of the hurricane (south coast) tend to be of lower stature, exhibiting more resistance to winds. All these reasons resulted in higher ΔNPV on the eastern side.

With a pinhole eye, hurricane María was more powerful, because the storm around the eye spun more quickly (Shen 2006). As hurricane María moved towards Puerto Rico, it underwent an eyewall replacement. The outer eyewall become dominant when hurricane María made landfall (Pasch, Penny, and Berg, 2018). The strongest wind and intense rainfall are usually found in the eyewall and to the right of the storm path on the northern hemisphere (Stanturf, Goodrick, Outcalt, 2007; Negrón Juárez et al., 2014). Negrón Juárez et al. (2014) suggested a possible

association between disturbance severity and wind speed. In this study, we hypothesized that high wind speeds over a certain threshold caused massive forest disturbance, and the forest disturbance lessened as the wind speed decreased along the storm track (Ayala-Silva and Twumasi, 2004; Oswalt and Oswalt, 2008; Boose, Serrano, and Foster, 2004).

Most of the highly affected forests were within 40 km of the landfall of hurricane María. The same trend was previously observed during hurricane Katrina, and approximately 90% of its effect was within 100 km of the coast (Stanturf, Goodrick, Outcalt, 2007).

6.3 Forest Structure and wind disturbance

Past studies have shown that forest disturbances from hurricanes vary by forest types (Negrón Juárez et al., 2014; Boose, Foster, and Fluet, 1994; Urquiza-Haas, Dolman, and Peres, 2007). Our results also verified that the Landsat-derived forest disturbance was sensitive to forest types in Puerto Rico. The least-resistant forest types analyzed in this study —Elfin and Sierra Palm cloud forests; Sierra Palm, transitional, and tall cloud forests (Fig. 12); mangrove forests; and seasonal evergreen forests with coconut palm—were in an agreement with previous research (Zimmerman et al., 1994; Brokaw and Grear, 1991; Lugo and Frangi, 2016; Lugo, 2008;). Mangrove trees with large diameters at breast height (d.b.h) experienced greater mortality than smaller trees (Lugo, 2008). Stem density, forest adaptation, the depth of the root system, and species shade tolerance resulted in the variance of the disturbance (Negrón Juárez et al., 2014; Zimmerman et al., 1994).

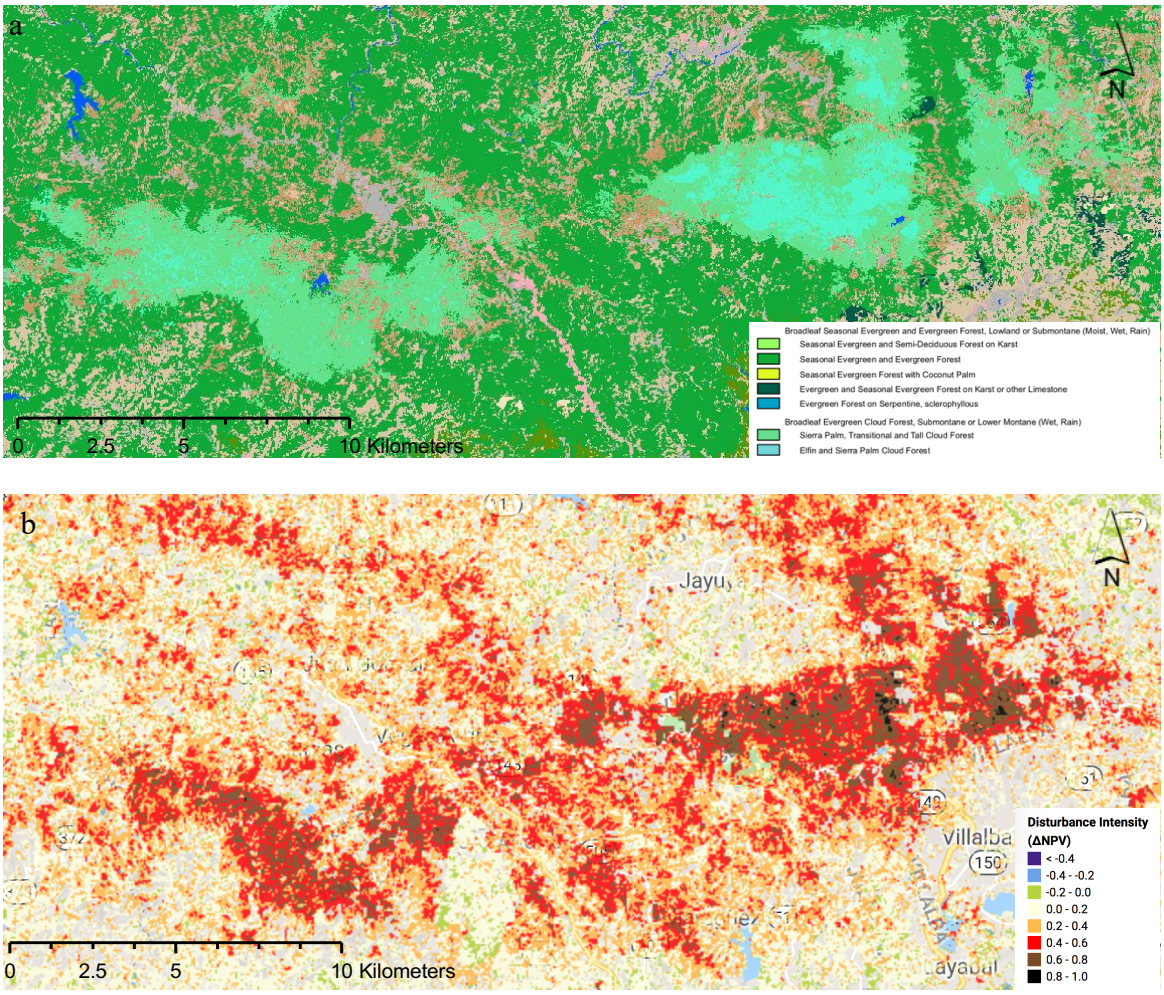

Fig. 12 The spatial distribution of the Elfin and Sierra Palm cloud forest and the Sierra Palm in transitional and tall cloud forest displayed in forest map (a) is similar to the pattern of (b) high forest disturbance (shown in red, brown, and black colors) in Toro Negro Commonwealth Forest, centered at 18.16°N, 66.65°W. Forest type map (a) provided by Kennaway et al. 2007 and Helmer et al. 2008.

Large older falling tree can cause successive uprooting and breaking of neighboring trees, causing such a domino effect (Maser et al. 1988), which might explain their higher ΔNPV. Protected forest types, including forests on serpentine substrate, mangroves, cloud forests, and *Pterocarpus* swamp, were mostly old (Kennaway and Helmer, 2007). Approximately 62–100%

of these forests were in the oldest age class (55–64+) in 2000. The mangroves in Puerto Rico were in the oldest age class (Kennaway and Helmer, 2007). Forests on more accessible and arable land at low to intermediate elevation tended to be younger (Kennaway and Helmer, 2007; Helmer, 2000), which may explain the large variance in the disturbance.

6.4 Forest Effect Tool

Our results showed that remote sensing images successfully captured the hurricane disturbance pattern in Puerto Rico. Google Earth Engine provided a highly functional platform to identify and process Landsat 8 images easily and conduct the full-spectral analysis quickly to analyze the effects of extreme weather events on land. Through GEE, we can disseminate our results to colleagues who share the same interests, policymakers, field workers, and NGOs (Gorelick et al., 2017). We also built user-interactive webpages through GEE, so that the general public can also access the data and maps.

The tool we developed combines data capability, image processing, and remote sensing process together, which enabled the further applications in rapid assessment of effects of hurricanes on

- Forest disturbance
- Road accessibility
- Identification of most affected residential area
- Ecosystem effects
- Forest recovery

This tool builds a workflow can be easily modified to update the analysis when more cloud free images become available. The same imagery processing steps and remote sensing methodology will allow us to assess forest vulnerability to repeated hurricanes.

7 Conclusion

This research showed a remote sensing and statistical analysis of the hurricane disturbance in Puerto Rico, and its association with the landform characteristics and forest structures. It shows the power of remote sensing for large-scale post-hurricane analysis and provides insights impossible to achieve from isolated ground efforts. Large portions of the disturbed forests were clustered in Luquillo Mountains, the lower mid-west forested area of the main island, and Piñones Mangroves in northeast of the main island. The factors of elevation, slope, windwardness, forest canopy height, distance to the hurricane track, distance to the hurricane landfall, forest type, forest age, and green vegetation ratio had significant effects on the spatial pattern and severity of the forest disturbance. Future projections indicate more frequent and intense extreme weather events (Knutson et al. 2010, Patricola and Wehner 2018). Therefore, the assessment of tree impacts and forest recovery are important areas of continued research. This study establishes a baseline for the rapid assessment of forest disturbances and spatial patterns in extreme weather. Improvements to the assessment of tree mortality from hurricanes can be obtained by including the observed field data.

8 Acknowledgement

This research was supported as part of the Next Generation Ecosystem Experiments-Tropics (NGEE), funded by the U.S. Department of Energy, Office of Science, Office of Biological and Environmental Research under contract number DE-AC02-05CH11231. We give special thanks

to Ariel E. Lugo from International Institute of Tropical Forestry, who provides helpful comments and suggestions to improve and clarify our manuscript. G-LiHT aerial photos of Puerto Rico were acquired in 2017/2018 Puerto Rico campaign, as part of the Department of Energy's NGEE Tropics project and NASA's Florescence Airborne Research Experiment (FLARE).

Declarations of interest:

The authors declare that they have no known competing financial interests or personal relationships that could have appeared to influence the work reported in this paper.

Bibliography

Adams, J. B., Sabol, D. E., Kapos, V., Almeida Filho, R., Roberts, D. A., Smith, M. O., & Gillespie, A. R. (1995). Classification of multispectral images based on fractions of endmembers: Application to land-cover change in the Brazilian Amazon. *Remote sensing of Environment*, 52(2), 137-154.

Adams, J. B., & Gillespie, A. R. (2006). *Remote sensing of landscapes with spectral images: A physical modeling approach*. Cambridge University Press.

Arriaga, L. (2000). Types and causes of tree mortality in a tropical montane cloud forest of Tamaulipas, Mexico. *Journal of Tropical Ecology*, 16(5), 623-636.

Ayala-Silva, T., & Twumasi, Y. A. (2004). Hurricane Georges and vegetation change in Puerto Rico using AVHRR satellite data. *International Journal of Remote Sensing*, 25(9), 1629-1640.

Bellingham, P. J., & Tanner, E. V. J. (2000). The influence of topography on tree growth, mortality, and recruitment in a tropical montane forest. *Biotropica,* 32(3), 378-384.

Baumann, M., Ozdogan, M., Wolter, P.T., Krylov, A., Vladimirova, N. and Radeloff, V.C., (2014). Landsat remote sensing of forest windfall disturbance. *Remote sensing of environment*, 143, pp.171-179.

Boose, E. R., Foster, D. R., & Fluet, M. (1994). Hurricane impacts to tropical and temperate forest landscapes. *Ecological Monographs*, *64*(4), 369-400.

Boose, E. R., Serrano, M. I., & Foster, D. R. (2004). Landscape and regional impacts of hurricanes in Puerto Rico. *Ecological Monographs*, 74(2), 335-352.

Brokaw, N. V., & Grear, J. S. (1991). Forest structure before and after Hurricane Hugo at three elevations in the Luquillo Mountains, Puerto Rico. *Biotropica*, 386-392.

Brandeis TJ, Turner JA (2013) Puerto Rico's forests, 2009. Resour Bull. SRS-191. U.S. Department of Agriculture Forest Service, Southern Research Station, Asheville

Canham, C. D., Thompson, J., Zimmerman, J. K., & Uriarte, M. (2010). Variation in susceptibility to hurricane damage as a function of storm intensity in Puerto Rican tree species. *Biotropica*, 42(1), 87-94.

Chambers, J. Q., Fisher, J. I., Zeng, H., Chapman, E. L., Baker, D. B., & Hurtt, G. C. (2007). Hurricane Katrina's carbon footprint on US Gulf Coast forests. *Science*, 318(5853), 1107-1107. doi:10.1126/science.1148913.

Clark, D. B., Castro, C. S., Alvarado, L. D. A., & Read, J. M. (2004). Quantifying mortality of tropical rain forest trees using high-spatial-resolution satellite data. *Ecology Letters*, *7*(1), 52-59.

Coltin, B., McMichael, S., Smith, T., Fong, T., 2016. Automatic boosted flood mapping from satellite data. *Int. J. Remote Sens*. 37 (5), 993–1015.

Cook, B. D., L. W. Corp, R. F. Nelson, E. M. Middleton, D. C. Morton, J. T. McCorkel, J. G. Masek, K. J. Ranson, V. Ly, and P. M. Montesano. 2013. NASA Goddard's Lidar, Hyperspectral and Thermal (G-LiHT) airborne imager. Remote Sensing 5:4045-4066, doi:10.3390/rs5084045.

Duryea, M. L., & Kampf, E. L. I. A. N. A. (2007). *Wind and trees: lessons learned from hurricanes*. University of Florida, IFAS Extension.

Everham, E. M., & Brokaw, N. V. (1996). Forest damage and recovery from catastrophic wind. The botanical review, 62(2), 113-185.

Feng, Y., Negron-Juarez, R.I., Patricola, C.M., Collins, W.D., Uriarte, M., Hall, J.S., Clinton, N. and Chambers, J.Q., (2018). Rapid remote sensing assessment of impacts from Hurricane Maria on forests of Puerto Rico. PeerJ Preprints, 6, p.e26597v1.

Flynn, D. F., Uriarte, M., Crk, T., Pascarella, J. B., Zimmerman, J. K., Aide, T. M., & Caraballo Ortiz, M. A. (2010). Hurricane disturbance alters secondary forest recovery in Puerto Rico. *Biotropica*, 42(2), 149-157.

Foster, D. R., Fluet, M., & Boose, E. R. (1999). Human or natural disturbance: landscape-scale dynamics of the tropical forests of Puerto Rico. *Ecological applications*, 9(2), 555-572. doi:10.2307/2641144.

Fox, J. & Monette, G. (1992) Generalized collinearity diagnostics. *JASA*, 87, 178-183

Frolking, S., Palace, M. W., Clark, D. B., Chambers, J. Q., Shugart, H. H., & Hurtt, G. C. (2009). Forest disturbance and recovery: A general review in the context of spaceborne remote sensing of impacts on aboveground biomass and canopy structure. *Journal of Geophysical Research: Biogeosciences*, 114(G2). doi:10.1029/2008jg000911.

Furby, S. L., & Campbell, N. A. (2001). Calibrating images from different dates to 'like-value'digital counts. *Remote Sensing of Environment*, 77(2), 186-196.doi:10.1016/s0034-4257(01)00205-x.

Gannon, B. M., & Martin, P. H. (2014). Reconstructing hurricane disturbance in a tropical montane forest landscape in the Cordillera Central, Dominican Republic: implications for vegetation patterns and dynamics. *Arctic, antarctic, and alpine research*, 46(4), 767-776.

Gorelick, N., Hancher, M., Dixon, M., Ilyushchenko, S., Thau, D., & Moore, R. (2017). Google Earth Engine: Planetary-scale geospatial analysis for everyone. *Remote Sensing of Environment*, 202, 18-27. doi:10.1016/j.rse.2017.06.031.

Hansen, M. C., Potapov, P. V., Moore, R., Hancher, M., Turubanova, S. A. A., Tyukavina, A., ... & Kommareddy, A. (2013). High-resolution global maps of 21st-century forest cover change. *science*, 342(6160), 850-853. doi:10.1126/science.1244693.

Harris, N.L., Lugo, A.E., Brown, S. and Heartsill-Scalley, T., (2012). Luquillo experimental forest: research history and opportunities. *Experimental Forest and Range EFR-1. Washington, DC: USDA Forest Service*. 152 p., 1.

Helmer, E. H. (2000). The landscape ecology of tropical secondary forest in montane Costa Rica. *Ecosystems*, 3(1), 98-114.

Helmer, E., Ramos, O., López, T. D. M., Quinones, M., & Diaz, W. (2002). Mapping the forest type and land cover of Puerto Rico, a component of the Caribbean biodiversity hotspot. *Caribbean Journal of Science, Vol. 38, No. 3-4, 165–183.*

Helmer, E. H., Brandeis, T. J., Lugo, A. E., & Kennaway, T. (2008). Factors influencing spatial pattern in tropical forest clearance and stand age: implications for carbon storage and species diversity. *Journal of Geophysical Research: Biogeosciences*, 113(G2).

Helmer, E. H., Ruzycki, T. S., Wunderle Jr, J. M., Vogesser, S., Ruefenacht, B., Kwit, C., ... & Ewert, D. N. (2010). Mapping tropical dry forest height, foliage height profiles and disturbance type and age with a time series of cloud-cleared Landsat and ALI image mosaics to characterize avian habitat. *Remote Sensing of Environment*, 114(11), 2457-2473.

Hilker, T., Wulder, M. A., Coops, N. C., Seitz, N., White, J. C., Gao, F., ... & Stenhouse, G. (2009). Generation of dense time series synthetic Landsat data through data blending with MODIS using a spatial and temporal adaptive reflectance fusion model. *Remote Sensing of Environment*, 113(9), 1988-1999.

Holdridge, L.R. (1967). Life zone ecology. Tropical Science Center. San José, Costa Rica.

Huete, A., Didan, K., Miura, T., Rodriguez, E. P., Gao, X., & Ferreira, L. G. (2002). Overview of the radiometric and biophysical performance of the MODIS vegetation indices. *Remote sensing of environment*, 83(1-2), 195-213.

Huete, A. R., Didan, K., Shimabukuro, Y. E., Ratana, P., Saleska, S. R., Hutyra, L. R., ... & Myneni, R. (2006). Amazon rainforests green-up with sunlight in dry season. *Geophysical research letters*, 33(6). doi:10.1029/2005gl025583.

Irish, J. L., Resio, D. T., & Ratcliff, J. J. (2008). The influence of storm size on hurricane surge. *Journal of Physical Oceanography*, 38(9), 2003-2013.

James, G., Witten, D., Hastie, T., & Tibshirani, R. (2013). *An introduction to statistical learning* (Vol. 112). New York: springer.

Jarvis, A., H.I. Reuter, A. Nelson, E. Guevara. (2008). Hole-filled SRTM for the globe Version 4, available from the CGIAR-CSI SRTM 90m Database: http://srtm.csi.cgiar.org.

Justice, C. O., Vermote, E., Townshend, J. R., Defries, R., Roy, D. P., Hall, D. K., ... & Lucht, W. (1998). The Moderate Resolution Imaging Spectroradiometer (MODIS): Land remote sensing for global change research. *IEEE transactions on geoscience and remote sensing*, 36(4), 1228-1249. doi:10.1109/36.701075.

Kennaway, T., & Helmer, E. H. (2007). The forest types and ages cleared for land development in Puerto Rico. *GIScience & Remote Sensing*, 44(4), 356-382.

Kennedy, R. E., Yang, Z., & Cohen, W. B. (2010). Detecting trends in forest disturbance and recovery using yearly Landsat time series: 1. LandTrendr—Temporal segmentation algorithms. *Remote Sensing of Environment*, *114*(12), 2897-2910.

Knutson, T.R., McBride, J.L., Chan, J., Emanuel, K., Holland, G., Landsea, C., Held, I., Kossin, J.P., Srivastava, A.K. and Sugi, M., (2010). Tropical cyclones and climate change. *Nature geoscience*, 3(3), p.157.

Luo, W., Taylor, M. C., & Parker, S. R. (2008). A comparison of spatial interpolation methods to estimate continuous wind speed surfaces using irregularly distributed data from England and Wales. *International journal of climatology*, *28*(7), 947-959.

Lugo, A. E. (2008). Visible and invisible effects of hurricanes on forest ecosystems: an international review. *Austral Ecology*, *33*(4), 368-398.

Lugo, A., and Frangi, J. L. (2016). Long-term response of Caribbean palm forests to hurricanes. *Caribbean Naturalist Special issue no. 1*, *1*, 157-175.

Lugo, A.E., Waide, R.B., Willig, M.R., Crowl, T.A., Scatena, F.N., Thompson, J., Silver, W.L., McDowell, W.H. and Brokaw, N., (2015). Ecological paradigms for the tropics: old questions and continuing challenges. Oxford Scholarship Online. DOI: 10.1093/acprof:osobl/9780195334692.001.0001

Lugo, A.E., (2018). 'Immediate Ecological Effects', in *Social-Ecological-Technological Effects of Hurricane María on Puerto Rico: Planning for Resilience under Extreme Events*. Springer, pp. 15-18.

Mabry, C. M., Hamburg, S. P., Lin, T. C., Horng, F. W., King, H. B., & Hsia, Y. J. (1998). Typhoon Disturbance and Stand-level Damage Patterns at a Subtropical Forest in Taiwan. *Biotropica*, 30(2), 238-250.

Maser, C., Cline, S.P., Cromack Jr, K., Trappe, J.M. and Hansen, E., 1988. What we know about large trees that fall to the forest floor. *Maser, C., Tarrant, RF, Trappe, JM, Franklin, JF (Tech. Eds.), From the Forest to the Sea: A Story of Fallen Trees. USDA Forest Survey General Technical Report PNWGTR-229. Oregon*, p.153.

McNab, W. H., Greenberg, C. H., & Berg, E. C. (2004). Landscape distribution and characteristics of large hurricane-related canopy gaps in a southern Appalachian watershed. *Forest Ecology and Management*, 196(2-3), 435-447.

Miller, G., & Lugo, A. E. (2009). Guide to the ecological systems of Puerto Rico. IITF-GTR-35.

Miner, Sola, E. 2000. Historia de los Hurracanes en Puerto Rico. First Book Publishing of Puerto Rico, San Juan, Puerto Rico, USA.

Negrón Juárez, R., Baker, D. B., Zeng, H., Henkel, T. K., & Chambers, J. Q. (2010). Assessing hurricane-induced tree mortality in US Gulf Coast forest ecosystems. *Journal of Geophysical Research: Biogeosciences*, 115(G4). doi:10.1029/2009jg001221.

Negrón Juárez, R. I., Chambers, J. Q., Marra, D. M., Ribeiro, G. H., Rifai, S. W., Higuchi, N., & Roberts, D. (2011). Detection of subpixel treefall gaps with Landsat imagery in Central Amazon forests. *Remote Sensing of Environment*, 115(12), 3322-3328.

Negrón Juárez, R., Baker, D. B., Chambers, J. Q., Hurtt, G. C., & Goosem, S. (2014a). Multi-scale sensitivity of Landsat and MODIS to forest disturbance associated with tropical cyclones. *Remote sensing of environment*, 140, 679-689. doi:10.1016/j.rse.2013.09.028.

Negrón Juárez, R. I., Chambers, J. Q., Hurtt, G. C., Annane, B., Cocke, S., Powell, M., ... & Saatchi, S. S. (2014b). Remote sensing assessment of forest disturbance across complex

mountainous terrain: The pattern and severity of impacts of tropical cyclone Yasi on Australian rainforests. *Remote Sensing*, 6(6), 5633-5649.

Oswalt, S. N., & Oswalt, C. M. (2008). Relationships between common forest metrics and realized impacts of Hurricane Katrina on forest resources in Mississippi. *Forest Ecology and Management*, *255*(5-6), 1692-1700.

Pasch R. J., Penny A. B., and Berg R. (2018). National Hurricane Center Tropical Cyclone Report: Hurricane María. National Weather Service. AL152017

Patricola, C. M., & Wehner, M. F. (2018). Anthropogenic influences on major tropical cyclone events. Nature, 563(7731), 339.

Pekel, J. F., Cottam, A., Gorelick, N., & Belward, A. S. (2016). High-resolution mapping of global surface water and its long-term changes. *Nature*, *540*(7633), 418.

Pouteau, R., & Stoll, B. (2012). SVM selective fusion (SELF) for multi-source classification of structurally complex tropical rainforest. *IEEE Journal of Selected Topics in Applied Earth Observations and Remote Sensing*, 5(4), 1203-1212.

Powell, M. D. (1982). The transition of the Hurricane Frederic boundary-layer wind field from the open Gulf of Mexico to landfall. *Monthly Weather Review*, *110*(12), 1912-1932.

Philippopoulos, K., & Deligiorgi, D. (2012). Application of artificial neural networks for the spatial estimation of wind speed in a coastal region with complex topography. *Renewable Energy*, 38(1), 75-82.

R Core Team (2013). R: A language and environment for statistical computing. R Foundation for Statistical Computing, Vienna, Austria. URL http://www.R-project.org/.

Roberts, D. A., Smith, M. O., & Adams, J. B. (1993). Green vegetation, nonphotosynthetic vegetation, and soils in AVIRIS data. *Remote Sensing of Environment*, 44(2-3), 255-269.

Schwartz, N. B., Uriarte, M., DeFries, R., Bedka, K. M., Fernandes, K., Gutiérrez-Vélez, V., & Pinedo-Vasquez, M. A. (2017). Fragmentation increases wind disturbance impacts on forest structure and carbon stocks in a western Amazonian landscape. *Ecological Applications*, 27(6), 1901-1915. doi:10.1002/eap.1576.

Shen, W. (2006). Does the size of hurricane eye matter with its intensity? *Geophysical research letters*, 33(18).

Shimabukuro, Y. E., & Smith, J. A. (1991). The least squares mixing models to generate fraction images derived from remote sensing multispectral data. *IEEE Transactions on Geoscience and Remote Sensing*, 29, 16–20.

Simard, M., Pinto, N., Fisher, J. B., & Baccini, A. (2011). Mapping forest canopy height globally with spaceborne lidar. *Journal of Geophysical Research: Biogeosciences*, *116*(G4).

Stanturf, J. A., Goodrick, S. L., & Outcalt, K. W. (2007). Disturbance and coastal forests: a strategic approach to forest management in hurricane impact zones. *Forest Ecology and Management*, 250(1-2), 119-135.

Sturrock, H. J., Cohen, J. M., Keil, P., Tatem, A. J., Le Menach, A., Ntshalintshali, N. E., Sexton, J. O., & Gosling, R. D. (2014). Fine-scale malaria risk mapping from routine aggregated case data. *Malaria journal*, 13(1), 421.

Tan, B., Masek, J. G., Wolfe, R., Gao, F., Huang, C., Vermote, E. F., ... & Ederer, G. (2013). Improved forest change detection with terrain illumination corrected Landsat images. Remote Sensing of Environment, 136, 469-483.

Tanner, E. V. J., Kapos, V., & Healey, J. R. (1991). Hurricane effects on forest ecosystems in the Caribbean. *Biotropica*, 513-521.

Uriarte, M., Canham, C. D., Thompson, J., Zimmerman, J. K., & Brokaw, N. (2005). Seedling recruitment in a hurricane-driven tropical forest: light limitation, density-dependence and the spatial distribution of parent trees. *Journal of Ecology*, 93(2), 291-304.

Uriarte, M., Canham, C. D., Thompson, J., Zimmerman, J. K., Murphy, L., Sabat, A. M., ... & Haines, B. L. (2009). Natural disturbance and human land use as determinants of tropical forest dynamics: results from a forest simulator. *Ecological Monographs*, 79(3), 423-443.

Uriarte, M., Thompson, J. and Zimmerman, J.K., (2019). Hurricane María tripled stem breaks and doubled tree mortality relative to other major storms. *Nature communications*, 10(1), p.1362.

Urquiza-Haas, T., Dolman, P. M., & Peres, C. A. (2007). Regional scale variation in forest structure and biomass in the Yucatan Peninsula, Mexico: Effects of forest disturbance. *Forest Ecology and Management*, *247*(1-3), 80-90.

Walker, L. R., Voltzow, J., Ackerman, J. D., Fernandez, D. S., & Fetcher, N. (1992). Immediate Impact of Hurricance Hugo on a Puerto Rican Rain Forest. *Ecology*, 73(2), 691-694. doi:10.2307/1940775.

Walker, L. R. (1991a). Tree damage and recovery from Hurricane Hugo in Luquillo experimental forest, Puerto Rico. *Biotropica*, 379-385.

Walker, L. R. (1991b). Summary of the effects of Caribbean hurricanes on vegetation. *Biotropica*, *23*(4), 442-447.

Xi, W., Peet, R. K., Decoster, J. K., & Urban, D. L. (2008). Tree damage risk factors associated with large, infrequent wind disturbances of Carolina forests. *Forestry*, *81*(3), 317-334.

Xin, Q., Olofsson, P., Zhu, Z., Tan, B., & Woodcock, C. E. (2013). Toward near real-time monitoring of forest disturbance by fusion of MODIS and Landsat data. *Remote Sensing of Environment*, *135*, 234-247.

Zeng, H., Chambers, J. Q., Negrón Juárez, R. I., Hurtt, G. C., Baker, D. B., & Powell, M. D. (2009). Impacts of tropical cyclones on US forest tree mortality and carbon flux from 1851 to 2000. *Proceedings of the National Academy of Sciences*, pnas-0808914106.

Zhu, Z., Woodcock, C.E. and Olofsson, P., 2012. Continuous monitoring of forest disturbance using all available Landsat imagery. *Remote sensing of environment*, 122, pp.75-91.

Zimmerman, J. K., Everham III, E. M., Waide, R. B., Lodge, D. J., Taylor, C. M., & Brokaw, N. V. (1994). Responses of tree species to hurricane winds in subtropical wet forest in Puerto Rico: implications for tropical tree life histories. *Journal of Ecology*, 911-922.